



# CHORUS

This is the accepted manuscript made available via CHORUS. The article has been published as:

## High-temperature phonon stabilization of $\gamma$ -uranium from relativistic first-principles theory

Per Söderlind, B. Grabowski, L. Yang, A. Landa, T. Björkman, P. Souvatzis, and O. Eriksson

Phys. Rev. B **85**, 060301 — Published 29 February 2012

DOI: [10.1103/PhysRevB.85.060301](https://doi.org/10.1103/PhysRevB.85.060301)

# High-temperature phonon stabilization of $\gamma$ -uranium from relativistic first-principles theory

Per Söderlind, B. Grabowski, L. Yang, and A. Landa  
*Lawrence Livermore National Laboratory, Livermore, California 94550, USA*

T. Björkman  
*COMP/Department of Applied Physics, Aalto University, FI-00076 Aalto, Finland*

P. Souvatzis and O. Eriksson  
*Department of Physics and Astronomy, Division of Materials Theory,  
Uppsala University, SE-751210 Uppsala, Sweden*  
(Dated: January 25, 2012)

A microscopic explanation for temperature stabilization of the body-centered cubic (bcc) phase in the actinide metals is proposed. We show that for a prototype actinide, uranium, phonon-phonon interaction promotes bcc  $\gamma$ -U when heated even though at low temperatures it is mechanically a strongly unstable phase. Utilizing the recently developed self-consistent *ab initio* lattice dynamics (SCAILD) scheme in conjunction with highly accurate and fully relativistic density functional theory we obtain phonon dispersion and density of states that compare well with data acquired from inelastic neutron-scattering experiments. The investigation thus establishes that high-temperature lattice dynamics can be modeled from *ab initio* theory even for complex materials with substantial electron correlation including the actinides.

PACS numbers:

Density-functional theory (DFT)<sup>1</sup> has proven to be remarkably successful in describing the  $T = 0$  K ground-state phases of most metals. Skriver<sup>2</sup> showed that it predicts the correct ground-state crystal structure for many transition elements when applied in a spherical linear muffin-tin orbital technique. Later<sup>3</sup> it became evident that DFT—implemented in more sophisticated methods appropriately treating complex crystal structures—also confirms the ground-state phases of the actinides. Except for metals with strong electron-correlation effects, such as the rare-earths, the DFT workhorse can nowadays be effectively used throughout the Periodic Table of Elements for *low-temperature* condensed-matter applications.

There has been a long-standing difficulty, however, to model *high-temperature* phases with an accuracy analogous to that of the ground state at room or lower temperatures. The reason is that treating electronic and vibrational interactions simultaneously within a quantum-mechanical framework is a daunting task. It becomes particularly problematic when the high-temperature phase is mechanically unstable at low temperatures thus ruling out the typically applied perturbation theory of the zero-temperature electronic structure. An additional and potentially serious pitfall, when studying *f*-electron systems such as the actinide or rare-earth metals, is the possibility of a dramatic change in the *f*-electron behavior with temperature. For instance, cerium metal has a temperature-driven ( $\alpha \rightarrow \gamma$ ) phase transition that has been argued to be caused by localization (Mott transition)<sup>4</sup> where the *f* states are removed from the Fermi level (highest occupied energy). Similarly, uranium (or any other actinide metal) could exhibit a localization of the *5f* shell at elevated temperatures that cannot be addressed within conventional DFT. Localization is consistent with the formation of a high-symmetry phase such as bcc in U (see below) but because there is no significant volume expansion, often observed during this type of transition, we have reason to believe that this difficult-to-model mechanism is not present in this case. It was also shown that localization did not play a role in stabilizing bcc in Pu<sup>5</sup>, a metal with undisputedly more electron correlation than uranium<sup>6</sup>.

Quantum-mechanical molecular-dynamics methods provide, in principle, the solution to the high-temperature problem but are feasible only if an accurate electronic structure can be calculated expeditiously enough. Meanwhile, an efficient methodology has been devised that couples DFT forces with temperature-driven atomic displacements (phonons). This self-consistent *ab initio* lattice dynamics (SCAILD) technique<sup>7</sup> has been used to investigate the high-temperature bcc phase of several metals including Ti, Zr, Hf, and even iron<sup>8</sup>. The approach has been described in detail<sup>9</sup> and has heretofore utilized *ab initio* forces obtained from the projector augmented wave (PAW) method in conjunction with the currently most robust PAW implementation, the Vienna *ab initio* simulation package (VASP)<sup>10</sup>. This method allows for efficient evaluation of the forces required for the SCAILD scheme while being adequately accurate for several transition metals. Here, however, we are concerned with a member of the actinides series, uranium. The actinides are heavy metals that are more challenging for electronic-structure theory for several reasons. In particular, the presence of narrow *5f*-electron states in the vicinity of the Fermi level strongly destabilizes symmetrical crystal structures, such as cubic or hexagonal, while giving rise to enhanced electron correlation and relativistic effects<sup>11,12</sup>.

In this context, the appearance of a high-symmetry cubic (bcc) phase between 1050-1410 K in U is non intuitive and hitherto not understood on a microscopic level. We mentioned it could be driven by electron localization that eliminates the mechanism destabilizing high-symmetry structures<sup>11</sup> but it may likewise arise from phonon-phonon interaction in analogy to the behavior found for Ti, Zr, and Hf<sup>7</sup> (or a combination of the two). It is the latter explanation that we explore in this study.

PAW calculations<sup>13</sup> are suitable for the lattice-dynamics scheme and appear to reproduce all-electron results<sup>14</sup> for the  $\alpha$ -U ground state in spite of its complex electronic structure. However, for temperatures close to the melting point where  $\gamma$ -U is stable, this approach<sup>13</sup> demonstrates discrepancies of over 40% with all-electron results. The PAW bulk modulus is 176 GPa<sup>13</sup> whereas the present FPLMTO calculations give 123 GPa. For comparison, laser-heated diamond anvil cell measurements show a bulk modulus of 113 GPa for  $\gamma$ -U<sup>15</sup>. Although a combination of a plane-wave technique and spin-orbit (SO) coupling is in principle possible and for lead apparently reasonable<sup>16</sup>, in practice it yields qualitatively wrong results for uranium. Specifically, inclusion of SO coupling lowers the equilibrium volume of  $\gamma$ -U<sup>13</sup>, although physically and as confirmed by all-electron calculations<sup>17</sup>, it expands the volume. Our own PAW (VASP, 14 valence electrons with PBE<sup>18</sup> exchange and correlation) examination including SO coupling does not reproduce the all-electron results for uranium (not shown) and we therefore omit them from the following discussion.

Considering the uncertainties regarding the PAW technique for U, we explore an electronic-structure method which—at the expense of computational burden—is highly accurate and suitable for actinide materials, the full-potential linear muffin-tin orbitals (FPLMTO) method. The specific version<sup>19</sup> has been applied successfully to  $T = 0$  K properties of actinides in the past<sup>3</sup>. It does not constrain the shapes of the charge density nor the potential. Furthermore, SO coupling is included in a first-order variational procedure for the valence  $d$  and  $f$  states<sup>20</sup>, while core states are treated with the fully relativistic Dirac equation. Most computational parameters are the same as those used in our calculation of uranium elastic constants<sup>14</sup>. The effects of orbital polarization (OP)<sup>21</sup> are examined because of their importance for the neighboring metals Np and Pu<sup>22</sup>. For the electron exchange and correlation we apply the generalized gradient approximation and all calculations are conducted at the theoretical zero-temperature equilibrium atomic volume, 20.85 Å<sup>3</sup>.

The SCAILD method can be viewed as a generalization of the frozen phonon method<sup>23</sup> and we therefore begin with evaluating the electronic-structure techniques for select zone-boundary (ZB) phonons applying the frozen-phonon approach. In Table I we show results obtained for the H- and N-point ( $T_2$  branch) ZB phonons. At zero temperature both are unstable resulting in imaginary frequencies (shown as negative). Notice that the FPLMTO results are substantially different to those obtained from PAW and that in all cases the former suggest a lesser degree of instability. For instance, for the H-point phonon at 300 K the PAW frequency is about twice that of the FPLMTO (both with no SO coupling). Including SO and OP increases the difference to a consequential factor of 2.5. The same trend holds true also for the  $T_2$  N-point phonon albeit less pronounced. Increasing the electronic temperature to 1200 K (Fermi-Dirac broadening and electronic entropy) diminishes the instability somewhat but does not remove the discrepancy between the methods. Hence, we conclude that even the currently most robust PAW implementation is not pertinent for uranium as it significantly overestimates the strength of the bcc instability. In fact, present SCAILD-PAW calculations (details below) fail to correctly stabilize bcc uranium below the melting temperature presumably because the electronic structure is too unstable to be properly counterbalanced by the phonon-phonon interactions provided within SCAILD.

Next, we tackle the high-temperature description of  $\gamma$ -U with SCAILD and the FPLMTO electronic structure. We are faced with two serious challenges: First, the forces in local-basis methods such as FPLMTO are numerically highly difficult to evaluate using a linear-response ansatz (Hellmann-Feynman forces), as opposed to the case of plane-wave techniques. Second, spin-orbit interaction and orbital polarization are practically incompatible with a linear-response force calculation, as the corresponding methodology is currently not thoroughly developed. We are, however, able to circumvent these issues by proceeding in analogy with the frozen-phonon approach. In particular, we choose to extract forces from (electronic) free-energy shifts due to small atomic displacements. The SCAILD scheme requires forces on all atoms in a supercell for which the atoms are thermally displaced from the perfect bcc lattice positions<sup>9</sup>. We obtain these forces by independently moving each atom a small amount ( $\pm 0.2\%$  of lattice constant) along the x, y, and z Cartesian axis, least-square fitting a second order polynomial to the free energies and extracting the force component along the considered axis. Because of the considerable computational effort by the all-electron method and the aforementioned displacement procedure we limit ourselves to study a  $3 \times 3 \times 3$  bcc supercell (27 atoms). A larger cell is of course preferred but our investigation for titanium (not shown) suggests that using a 27-atom supercell in lieu of a larger cell is reasonable when focusing on the phonon dispersion and density of states.

In Fig. 1 we show the SCAILD phonon dispersions at 500 K (bcc is experimentally unstable) for the FPLMTO treatment with (black line) and without (black line solid squares) spin-orbit interaction (including OP changes the dispersion a small amount, not shown) together with PAW results (red line solid circles). Clearly, PAW gives the strongest unstable dispersions, particularly the  $\Gamma$ -H branch is very negative as a result of too soft H-point phonons. The FPLMTO with SO is still unstable at 500 K but the instability regions are much smaller. The scalar relativistic

(noSO) all-electron result is also less unstable suggesting that an inaccurate PAW potential influences the phonon as suggested also by our frozen-phonon analysis (Table I). Here we apply the library VASP PBE PAW, but it may be possible to improve on it by including deeper lying core electrons in the potential. However, the problem with SO still remains and no further optimization of the PAW are attempted.

Our principal result is the stable phonon dispersion at 1113 K (neutron-scattering data<sup>24</sup> exist at this temperature) obtained from FPLMTO free-energy computations coupled with SCAILD. In Fig. 2 we display our data that serve as predictions since no experimental phonon dispersion exist for  $\gamma$ -U even though bcc is the stable phase at this temperature. Armed with this outcome we are able to predict the equation-of-state for high-temperature  $\gamma$ -U by constructing a free energy inclusive of the temperature-dependent lattice contributions. In practice the calculations need to be undertaken on a grid of volumes and temperatures so that the phase space is sufficiently sampled<sup>25</sup>. We note, however, that the phonon dispersion is rather insensitive to temperature in the 1100-1300 K range (not shown) which is entirely consistent with the experimental work<sup>24</sup>. In the absence of a measured  $\gamma$ -U phonon dispersion, we instead compare our calculated phonon density of states with that collected from inelastic neutron-scattering<sup>24</sup> in Fig. 3. The two-peak feature of the measured spectra is clearly reproduced while the intensity and location of the high energy peak is identical (no scaling is being applied). At the lowest energies, the disagreement is due to the non-linearity of some branches near zero and a too soft ( $T_1$ )  $\Gamma$ -N phonon branch, in analogy with Ti, Zr, and Hf<sup>7</sup>. The reason for this may be the application of a too small supercell, not sufficiently strong SCAILD phonon-phonon interaction, or not accurate enough DFT electronic structure.

In conclusion, we have calculated high-temperature phonons for a prototype actinide metal from relativistic first-principles theory. In spite of being strongly unstable at low temperatures, the vibrational entropy introduced through SCAILD, coupled with forces extracted from FPLMTO free-energy calculations, produces a mechanically stable phase with a phonon dispersion that is compatible with observations. The corresponding phonon density of states agrees satisfactorily with inelastic neutron-scattering experiments, but also reveals that low-energy phonon modes may be underestimated similarly to what was found in Ti, Zr, and Hf<sup>7</sup> suggesting that the SCAILD approach does not include all anharmonicity or that a larger computational supercell is required. Spin-orbit and orbital-polarization correlations together with a robust all-electron potential predict a rather plausible behavior of  $\gamma$ -U at lower temperatures and are essential for a realistic high-temperature description. Hence, the enigmatic stability of the high-symmetry bcc structure of U, and likely the remaining actinides, finds its explanation as being due to phonon-phonon interactions.

We have applied a methodology that circumvents the numerical difficulties of calculating linear-response forces by using free-energy changes due to small atomistic displacements. This is important because it now allows the use of SCAILD for any complex material for which a realistic energy can be evaluated. One example is plutonium metal<sup>26</sup> and we envision to apply the present methodology in the near future to study important anomalous temperature-dependent properties for this metal.

### Acknowledgments

Computing support for this work came from the LLNL Computing Grand Challenge program. O. E. acknowledges support from VR, KAW, and ERC (grant 247062). We thank M. Manley for discussions. This work performed under the auspices of the U.S. DOE by LLNL under Contract DE-AC52-07NA27344.

- 
- <sup>1</sup> P. Hohenberg and W. Kohn, Phys. Rev. **136**, B864 (1964); W. Kohn and L. Sham, Phys. Rev. **140**, A1133 (1965).
  - <sup>2</sup> H. L. Skriver, Phys. Rev. B **31**, 1909 (1985).
  - <sup>3</sup> P. Söderlind, Adv. Phys. **47**, 959 (1998).
  - <sup>4</sup> B. Johansson, Philos. Mag. **30**, 469 (1974).
  - <sup>5</sup> X. Dai, S. Y. Savrasov, G. Kotliar, A. Migliori, H. Ledbetter, and E. Abrahams, Science **300**, 953 (2003); G. Kotliar and D. Vollhardt, Phys. Today **57**, 53 (2004).
  - <sup>6</sup> R. J. McQueeney, A. C. Lawson, A. Migliori, T. M. Kelley, B. Fultz, M. Ramos, B. Martinez, J. C. Lashley, and Sven C. Vogel, Phys. Rev. Lett. **92**, 146401 (2004).
  - <sup>7</sup> P. Souvatzis, O. Eriksson, M. I. Katsnelson, and S. P. Rudin, Phys. Rev. Lett. **100**, 095901 (2008).
  - <sup>8</sup> W. Luo, B. Johansson, O. Eriksson, S. Arapan, P. Souvatzis, M. I. Katsnelson, and R. Ahuja, PNAS **107**, 9962 (2010).
  - <sup>9</sup> P. Souvatzis, O. Eriksson, M. I. Katsnelson, and S. P. Rudin, Comput. Matter. Sci. **44**, 888 (2009).
  - <sup>10</sup> G. Kresse and J. Furthmüller, Phys. Rev. B **54**, 11169 (1996).
  - <sup>11</sup> P. Söderlind, O. Eriksson, B. Johansson, J. M. Wills, and A. M. Boring, Nature **374**, 524 (1995).
  - <sup>12</sup> P. Söderlind, G. Kotliar, K. Haule, P. M. Oppeneer, and D. Guillaumont, MRS Bull. **35**, 883 (2010).
  - <sup>13</sup> C. D. Taylor, Phys. Rev. B **77**, 094119 (2008).

- <sup>14</sup> P. Söderlind, Phys. Rev. B **66**, 085113 (2002).
- <sup>15</sup> C. -S. Yoo, H. Cynn, and P. Söderlind, Phys. Rev. B **57**, 10359 (1998).
- <sup>16</sup> A. D. Corso, J. of Phys.: Condens. Matter **20**, 445202 (2008); M. J. Verstraete, M. Torrent, F. Jollet, G. Zerah, and X. Gonze, Phys. Rev. B **78**, 045119 (2008).
- <sup>17</sup> M. S. S. Brooks, J. Phys. F **13**, 103 (1983); P. Söderlind, L. Nordström, L. Yongming, and B. Johansson, Phys. Rev. B **42**, 4544 (1990).
- <sup>18</sup> J. P. Perdew, K. Burke, M. Ernzerhof, Phys. Rev. Lett. **78**, 1396 (1997).
- <sup>19</sup> J. M. Wills, O. Eriksson, M. Alouani, and D. L. Price, in *Electronic Structure and Physical Properties of Solids*, edited by H. Dreysse (Springer-Verlag, Berlin, 1998), p. 148; J. M. Wills, M. Alouani, P. Andersson, A. Delin, O. Eriksson, and A. Grechnev, *Full-Potential Electronic Structure Method, Energy and Force Calculations with Density Functional and Dynamical Mean Field Theory* (Springer Series in Solid-State Science) **167**, (2010).
- <sup>20</sup> L. Nordström, J. M. Wills, P. H. Andersson, P. Söderlind, O. Eriksson, Phys. Rev. B **63** 035103 (2000).
- <sup>21</sup> O. Eriksson, B. Johansson, and M. S. S. Brooks, J. Phys.: Condens. Matter **1**, 4005 (1989).
- <sup>22</sup> P. Söderlind, Phys. Rev. B **77**, 085101 (2008); P. Söderlind and A. Gonis, Phys. Rev. B **82**, 033102 (2010).
- <sup>23</sup> B. N. Harmon, W. Weber, and D. R. Hamann, Phys. Rev. B **25**, 1109 (1982).
- <sup>24</sup> M. E. Manley, B. Fultz, R. J. McQueeney, C. M. Brown, W. L. Hults, J. L. Smith, D. J. Thoma, R. Osborn, and J. L. Robertson, Phys. Rev. Lett. **86**, 3076 (2001).
- <sup>25</sup> P. Souvatzis, A. Arapan, O. Eriksson and M. I. Katsnelson, Europhys. Lett. **96**, 66006 (2011).
- <sup>26</sup> P. Söderlind and B. Sadigh, Phys. Rev. Lett. **92**, 185702 (2004).

## Figures

FIG. 1: (Color online). Phonon dispersions for  $\gamma$ -U at 500 K. SCAILD coupled with FPLMTO w/o spin-orbit interaction (black line solid squares), with SO (black solid line), and with VASP-PAW (red line solid circles).

FIG. 2: Phonon dispersion for  $\gamma$ -U at 1113 K. SCAILD coupled with FPLMTO (SO+OP).

FIG. 3: Phonon density of states for  $\gamma$ -U at 1113 K, calculated (solid line) and inelastic neutron-scattering data taken from Ref.<sup>24</sup>.

## Tables

TABLE I: H- and N-point ( $T_2$ ) ZB phonons for bcc U obtained from the frozen-phonon method<sup>23</sup> and electronic free energies corresponding to 300 K and 1200 K. The results are gathered from the FPLMTO method w/o (noSO), with spin-orbit coupling (SO), with orbital polarization (SO+OP), and from the PAW method (VASP-PAW). All frequencies ( $\nu = \omega/2\pi$ ) are in units of THz and we adopt the convention to display imaginary (unstable) frequencies as negative.

ZB phonon	noSO	SO	SO+OP	VASP-PAW
H (300 K)	-1.14	-0.91	-0.86	-2.03
H (1200 K)	-1.03	-0.68	-0.54	-1.94
N: $T_2$ (300 K)	-2.28	-2.16	-2.14	-2.64
N: $T_2$ (1200 K)	-2.17	-2.04	-2.01	-2.55

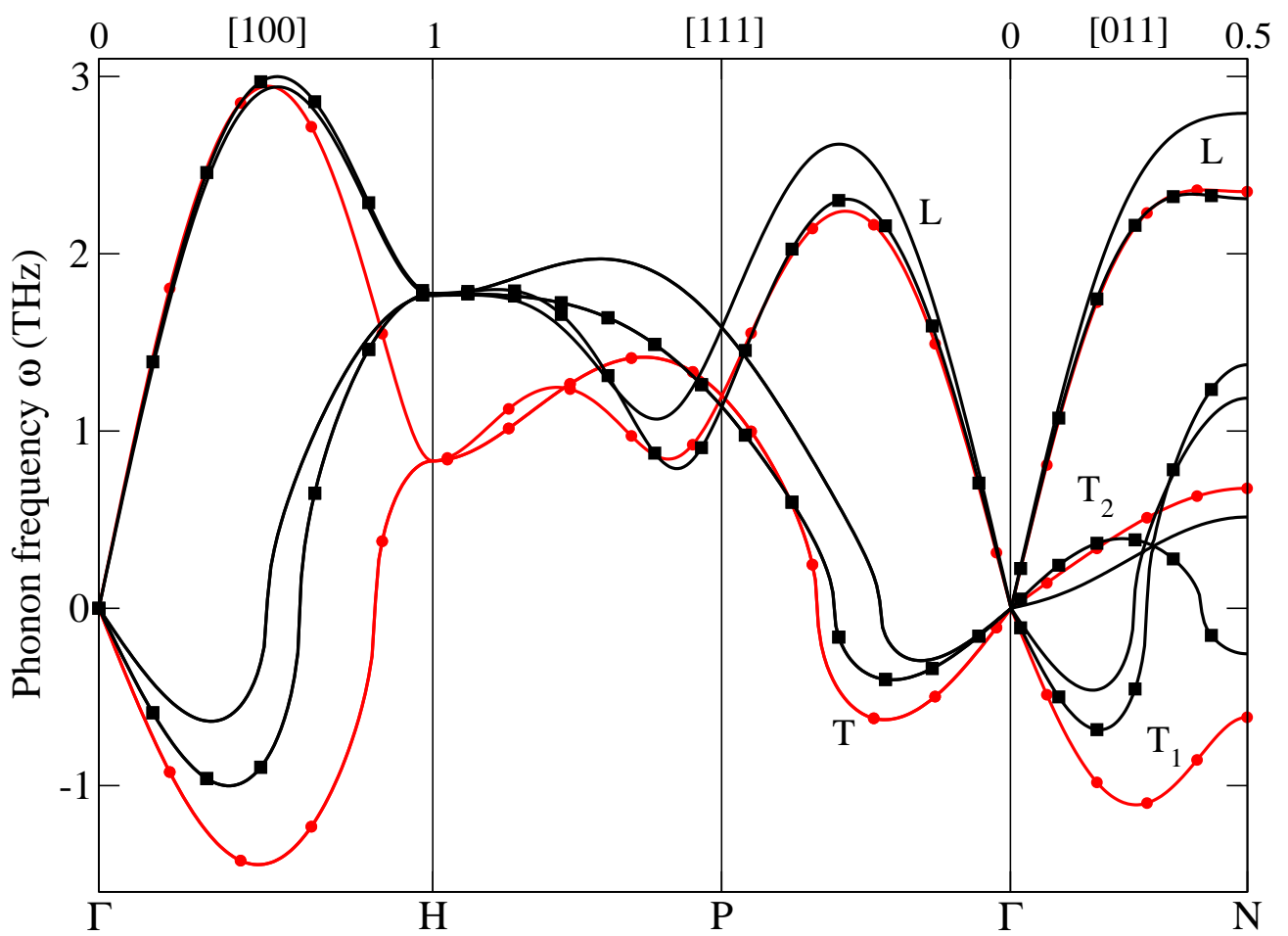


Figure 1

LN12728BR

25Jan2012

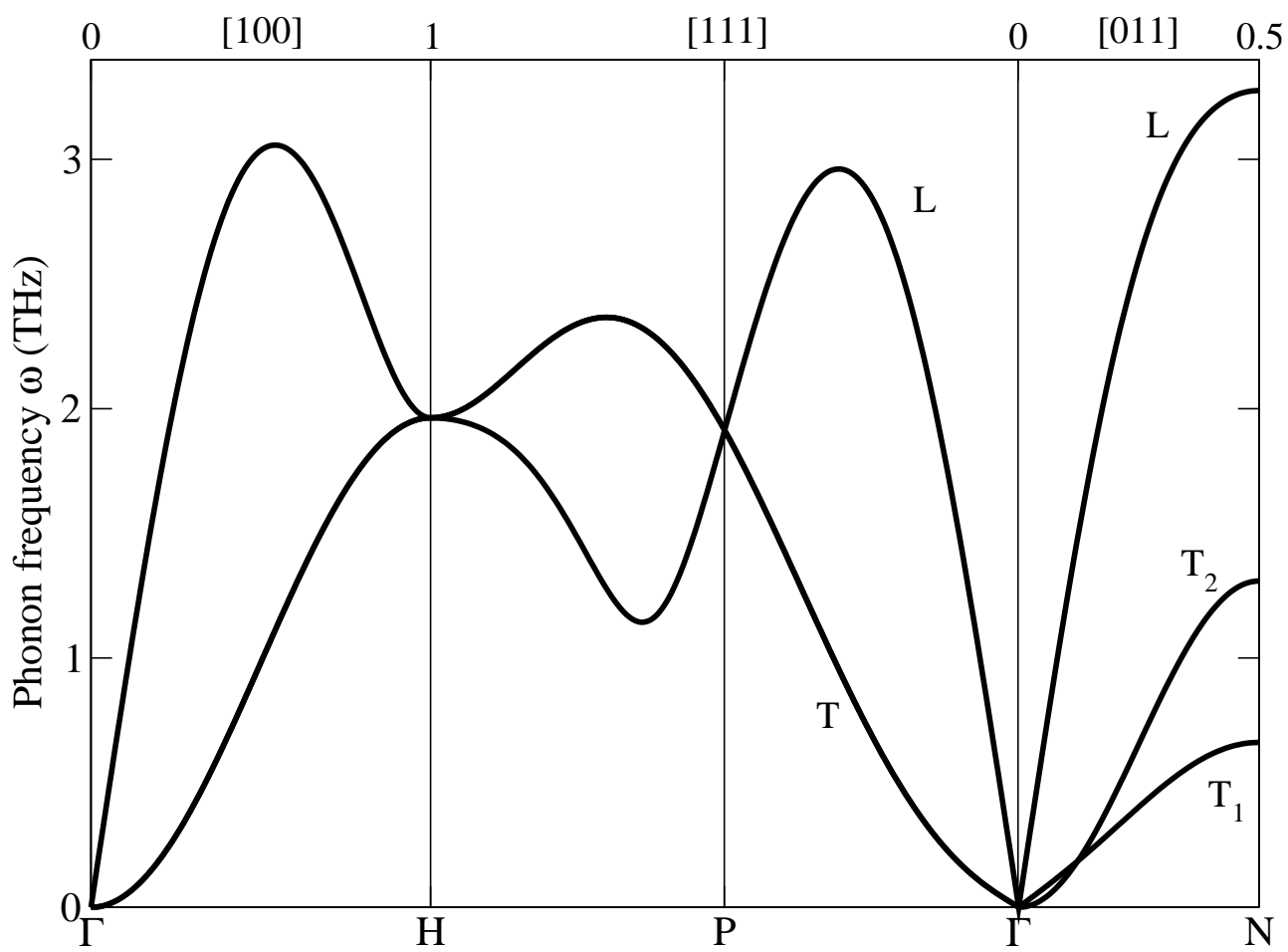


Figure 2 LN12728BR 25Jan2012

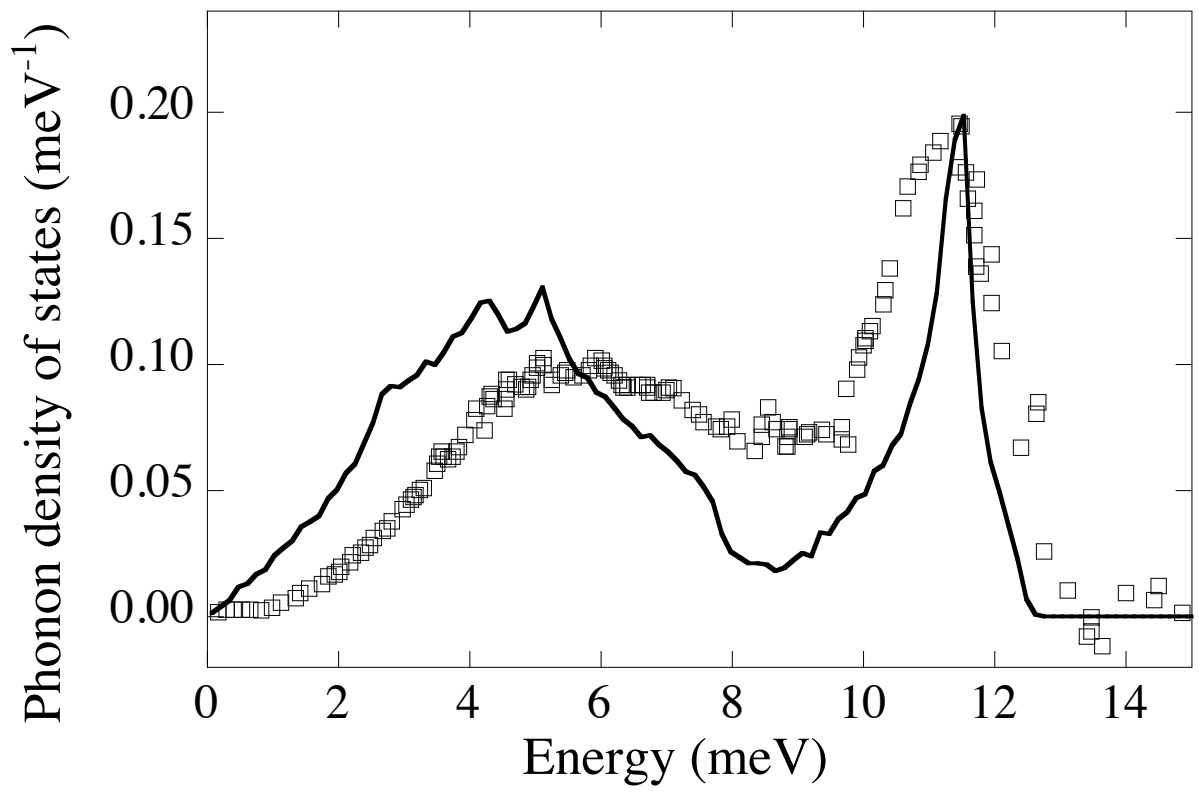


Figure 3

LN12728BR

25Jan2012